L x-ray fluorescence cross sections and intensity ratios in some high-Z elements excited by 23.62- and 24.68-keV photons

D. V. Rao
Dipartimento di Fisica, Università di Roma "La Sapienza," piazza Aldo Moro 2, 00185 Roma, Italy

R. Cesareo
Centro Interdipartimentale di Ricerca per L'Analisi dei Modelli e dell'Informazione nei Sistemi Biomedici, Università di Roma "La Sapienza," piazza Aldo Moro 2, 00185 Roma, Italy

G. E. Gigante
Dipartimento di Fisica, Università di Roma "La Sapienza," piazza Aldo Moro 2, 00185 Roma, Italy and Centro Interdipartimentale di Ricerca per L'Analisi deli Modelli e dell'Informazione nei Sistemi Biomedici, Università di Roma "La Sapienza," piazza Aldo Moro 2, 00185 Roma, Italy

(Received 3 August 1992)

Ll, $L\alpha$, $L\beta$, and $L\gamma$ x-ray fluorescence cross sections have been measured for the elements Pr, Ho, Yb, Au, and Pb using photon energies of 23.62 and 24.68 keV. Measurements have been performed using an x-ray tube with a secondary-exciter system as the excitation source. The secondary exciters of Cd and In were pure metals ($>99.9\%$). The x-ray tube with a secondary-target arrangement was used to obtain high intensity with a high degree of monochromatization. By using an x-ray tube, it is possible to measure x-ray fluorescence cross sections and ratios even for low-intensity x rays (Ll). Experimental results have been compared with the theoretically calculated values of L x-ray fluoresence cross sections. A fairly good correspondence is observed between experimental and calculated values. The intensity ratios for the intense transitions $I_{L\beta}/I_{L\alpha}$ are in good agreement with the calculated values.

PACS number(s): 32.80.Hd, 32.30.Rj

INTRODUCTION

Studies of the L x-ray fluorescence cross sections of many elements and their intensity ratios have been reported in the past [1–6]. Accurate determination of L x-ray fluorescence cross sections and their intensity ratios for different elements is important because of their wide use in the fields of atomic, molecular, and radiation physics, and in nondestructive elemental analysis of materials using either traditional photon sources or synchrotron radiation [7].

L x-ray fluorescence cross sections and their intensities can be calculated by using photoelectric cross sections, fluorescence yields, and fractional emission rates. Uncertainties in these tabulated quantities largely reflect the error in L x-ray fluorescence cross sections. For this reason most users prefer the experimental values of the cross sections whenever large discrepancies are observed between theoretical and experimental values. For quantitative analytical applications it is necessary to know the different relative intensities of the photons that contribute to the fluorescence. Since fluorescence cross sections increase as the energy decreases, the contributions to L x-ray fluorescence of low-energy, low-intensity transitions can be very important.

Earlier experimental L x-ray fluorescence cross sections and their intensity ratios were measured using radioisotopes as excitation sources. They have the advantages of stable intensity and energy and of small size, which allows compact and efficient geometry, and they operate without any external power. The drawbacks are the small number of suitable radioisotopes available at different excitation energies and the decline of intensity with time if the half-life is of the order of a few years or shorter, and the relatively low flux.

An alternative to radioisotopes is use of an x-ray tube with a secondary-target arrangement. In secondary-target arrangements, the primary radiation generated by the electrons is used to excite the secondary target. In this process, the major part of the bremsstrahlung radiation generated by the first target is eliminated and the radiation from the secondary target has a high degree of monochromatization with high intensity. The present measurements have been performed with an x-ray tube with a secondary-exciter system as the excitation source instead of radioisotopes. By using an x-ray tube it is possible to measure L x-ray fluorescence cross sections even for low intensity x rays ($L1$).

In addition, these measurements serve to provide a check on the theoretical calculations of some of the fundamental physical parameters, such as L-subshell ionization cross sections, fluorescence yields [8], Coster-Kronig transition probabilities [9], and radiative decay rates [10], the direct determination of which presents many difficulties.

The K x rays of Cd and In provided incident photons with energies of 23.62 and 24.68 keV, respectively. The choice of the incident energies was such that the K-shell electrons from the target element were not knocked out. The vacancies were therefore not transferred from the K to the L shell.

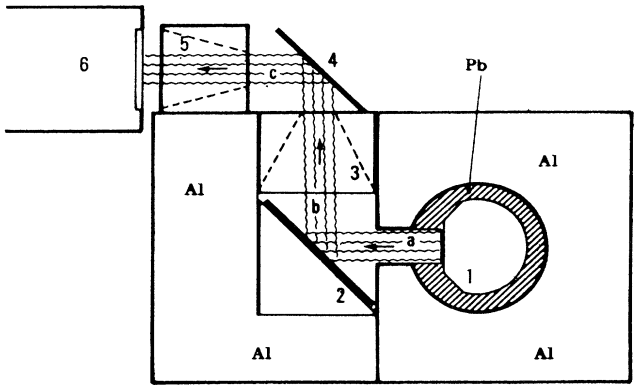

FIG. 1. Schematic of the setup of the apparatus employed for generating L x rays. 1, x-ray tube; 2, secondary target of element t; 3, conical collimator internally covered with a foil of element t; 4, sample; 5, conical collimator internally covered with a foil of element t; 6, detector. a labels primary bremsstrahlung radiation, b labels secondary radiation, and c labels L x rays emitted by the sample.

EXPERIMENTAL PROCEDURE

The primary radiation source consisted of an x-ray tube with a tungsten anode whose maximum high voltage and current are 80 kV and 5 mA, respectively. The x-ray spectrometer with a secondary-target arrangement and the geometry used are shown in Fig. 1. The figure also shows the energy distribution of the beam in the three main sections of the radiation path, i.e., at the exit of the x-ray tube, at the exit of the secondary collimator, and at the entrance of the detector. This geometry was adopted to reduce the contribution of photons scattered from the secondary target and then rescattered by the sample in to the detector. The effect of this geometry on the background radiation has been studied in earlier investigations [11,12]. To check the monochromaticity of the beam, a spectrum was taken directly from the x-ray tube with a Cd secondary target. More than 97% of the counts were found in the Cd x-ray peaks.

The secondary exciters of Cd and In were pure metals (>99.9%). The K x rays of Cd and In provided incident photons with energies of 23.62 and 24.68 keV, respectively. These energies were calculated by taking the weighted average of $K\alpha$ and $K\beta$ x-ray energies according to their intensity ratio [13]. The Au and Pb targets were in the form of circular discs having thicknesses of approximately 0.01 mm; spectroscopically pure (purity >99.9%) self-supporting Pr, Ho, and Yb samples of thicknesses ranging from 96 to 350 mg/cm^2 were used for the measurements.

The direct beam from the x-ray tube was incident on the secondary target. Fluorescent x rays produced in the secondary-target exit from the collimator excite the sample. The samples were placed at a 45° angle with respect to the direct beam, and fluorescent x rays emitted at 90° to the direct beam were detected by a collimated hyper-

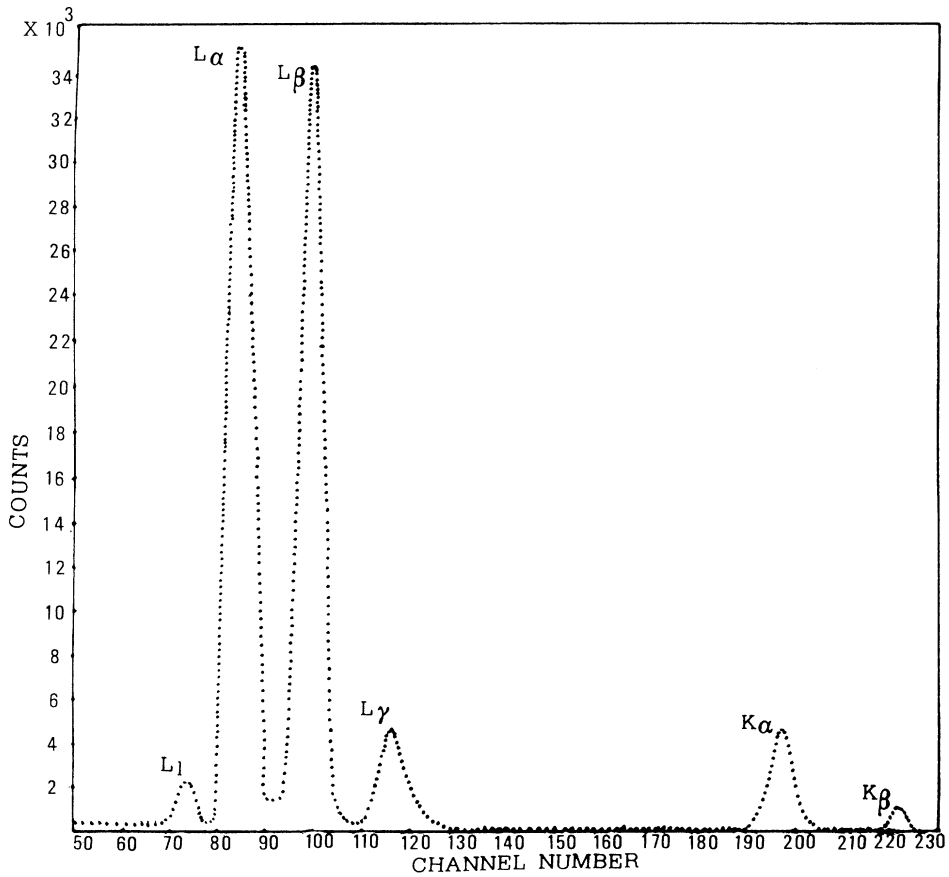

FIG. 2. Complete L x-ray spectrum of Au with a Cd secondary target.

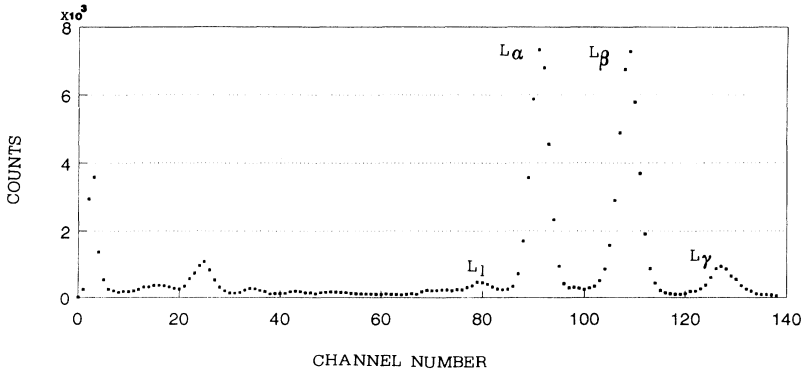

FIG. 3. L x-ray spectrum of Pb with a Cd secondary target after subtraction of the background.

pure Ge(Li) detector having a thickness of 5 mm and energy resolution of 160 eV at 5.9 keV. The amplified output pulses from this detector were fed into a 1024-channel computerized multichannel analyzer.

The complete spectrum of Au L x rays with a Cd secondary target is shown in Fig. 2. The bremsstrahlung continuum is completely absent in the other channels after the $L\gamma$ peak. A clear separation of $K\alpha$ and $K\beta$ peaks can be observed from the spectrum. However, various components of the L-shell x rays resulting from transitions of the electrons to the L subshell of the same element are very close to one another and are not separated due to the limited resolution of the spectrometer. Thus the number of L x rays counted under each peak may be due to transitions of electrons from M, N, and higher subshells to any of the three L subshells, depending on the energy of the x rays and the selection rule.

Three sets of measurements were made for each target for irradiation times of 1000 and 2000 s, and for both Cd and In exciters. A typical spectrum is shown in Fig. 3, after subtraction of the background. The stability of the spectrometer was monitored regularly before and after each set of runs by noting the number of counts from a Cu standard. To eliminate further any systematic error due to system instability or other effects, the three measurements of each sample were made on three different occasions well separated in time. The final spectra used were the weighted average of the three measurements.

DATA ANALYSIS

The experimental L x-ray fluorescence cross sections can be measured using

$$\sigma_{Li}^{x}=\frac{I_{Li}}{I_0(E_i)GT\epsilon_{Li}t} , \tag{1}$$

where I_{Li} is the observed intensity (area under the photopeak) corresponding to the Li group of x rays, I_0 is the intensity of the incident radiation, G is the geometrical factor, ϵ_{Li} is the detection efficiency for the Li group of x rays, and T is the self-absorption correction factor for the target material, which accounts for the absorption in the target of the incident photons and the emitted characteristic x rays. T was calculated using the relation

$$T=\frac{1-\exp[-h_z(E_i)t]}{h_z(E_i)} , \tag{2}$$

where

$$h_z(E_i)=\left[\frac{\mu_{\text{inc}}}{\cos(\theta_1)}+\frac{\mu_{\text{emit}}}{\cos(\theta_2)}\right] ,$$

where μ_{inc} and μ_{emit} are the absorption coefficients [14] in (cm^2/g) of incident photons and emitted characteristic x rays, respectively. The angles of incident photons and emitted x rays with respect to the normal at the surface of the sample, θ_1 and θ_2, were equal to 45° in the present setup, and t is the thickness of the target in g/cm^2. Thus, knowing the product $I_0G\epsilon_{Li}$, one can determine the absolute values of the x-ray fluorescence cross sections. However, the value of the factor $I_0G\epsilon_{Li}$, which contains the terms related to the incident-photon flux, the geometrical factor, and the absolute efficiency of the x-ray detector, was determined by collecting the K x-ray spectra of thin samples of Fe, Ni, Cu, Ga, Se, and Mo, and by using the relation

$$I_0G\epsilon_{K\alpha}=\frac{I_{K\alpha}}{\sigma_{K\alpha}T_{K\alpha}t} , \tag{3}$$

where the terms $I_{K\alpha}$, $T_{K\alpha}$, and $\epsilon_{K\alpha}$ have the same meaning as in Eq. (1), except that they correspond to K x-rays instead of the ith group of L x-rays. Theoretical values of ($\sigma_{K\alpha}$) x-ray fluorescence cross sections were calculated using the relation

$$\sigma_{K\alpha}=\sigma_K(E)\omega_K F_{K\alpha} , \tag{4}$$

where $\sigma_K(E)$ is the K-shell photoionization cross section [15] for the given element at the excitation energy E, ω_K is the K-shell fluorescence yield [7], and $F_{K\alpha}$ is the fractional x-ray emission rate for $K\alpha$ x-rays, defined as

$$F_{K\alpha}=\left[1+\frac{I_{K\beta}}{I_{K\alpha}}\right]^{-1} , \tag{5}$$

where $I(K\beta)/I(K\alpha)$ is the $K\beta$-to-$K\alpha$ x-ray intensity ratio [17]. Since the experimental values were not available for all elements, it was decided to use the theoretical values to evaluate $I_0G\epsilon(K\alpha)$. The experimental L-shell x-ray intensity ratios $I_{Li}/I_{L\alpha}$ were evaluated using the relation

$$\frac{I_{Li}}{I_{L\alpha}}=\frac{N_{Li}}{N_{L\alpha}}\frac{T_{L\alpha}}{T_{Li}}\frac{\epsilon_{L\alpha}}{\epsilon_{Li}} , \tag{6}$$

TABLE I. Comparison of L x-ray fluorescence cross sections (in b/atom) with calculated values at excitation energies E (keV).

		σ_{L1}		$\sigma_{L\alpha}$		$\sigma_{L\beta}$		$\sigma_{L\gamma}$	
Target	E	Expt.	Theor.	Expt.	Theor.	Expt.	Theor.	Expt.	Theor.
Pb	23.62	162±12	146.26	3442±264	2712.28	3540±256	2620.62	584±48	495.25
	24.68	136±11	108.80	2550±194	2017.68	2610±188	2001.90	484±38	380.20
Au	23.62	108±8.0	91.29	2240±186	1778.88	2342±192	1820.50	398±32	315.50
	24.68	98±7.8	81.27	1962±166	1583.20	2078±174	1644.60	347±29	285.25
Yb	23.62	38±3.2	30.75	832±68	680.89	946±78	772.80	178±12	146.32
	24.68	34±2.8	26.50	748±62	586.62	793±66	632.14	158±10	124.82
Ho	23.62	30±2.4	24.34	656±54	536.98	712±60	564.28	122±10	98.77
	24.68	26±2.2	21.12	583±48	465.60	625±52	500.25	108±8.0	88.00
Pr	23.62			288±24	233.13	304±25	240.85	53±3.4	41.75
	24.68			249±20	204.68	268±22	215.69	47±2.8	38.50

where $N(Li)$ and $N(L\alpha)$ represent the ratio of the counting rates under the Li and $L\alpha$ peaks, $T(L\alpha)/T(Li)$ is the ratio of the self-absorption correction factors of the target that accounts for the absorption of the incident K x rays and the emitted L x rays in the target material, and $\epsilon(L\alpha/\epsilon(Li)$ is the ratio of the detector-efficiency values for $L\alpha$ and Li x rays, respectively.

RESULTS AND DISCUSSION

The measured values of L x-ray fluorescence cross sections for Pr, Ho, Yb, Au, and Pb at different excitation energies are listed in Table I. The values of the L x-ray fluorescence cross sections are calculated from the theoretical subshell photoionization cross sections [15] and radiative decay rates [16,17], semiempirically fitted values [7] of fluorescence yields, and Coster-Kronig transition probabilities, using the following relations [18,19]:

$$\begin{aligned}
\sigma_{L1}^{x} &= (\sigma_{Ll} f_{13} + \sigma_{L1} f_{12} f_{23} + \sigma_{L2} f_{23} + \sigma_{L3})\omega_3 F_{3l} , \\
\sigma_{L\alpha}^{x} &= (\sigma_{L1} f_{13} + \sigma_{L1} f_{12} f_{23} + \sigma_{L2} f_{23} + \sigma_{L3})\omega_3 F_{3\alpha} , \\
\sigma_{L\beta}^{x} &= \sigma_{L1}\omega_1 F_{1\beta} + (\sigma_{L1} f_{12} + \sigma_{L2})\omega_2 F_{2\beta} \\
&\quad + (\sigma_{L1} f_{13} + \sigma_{L1} f_{12} f_{23} + \sigma_{L2} f_{23} + \sigma_{L3})\omega_3 F_{3\beta} , \\
\sigma_{L\gamma}^{x} &= \sigma_{L1}\omega_1 F_{1\gamma} + (\sigma_{L1} f_{12} + \sigma_{L2})\omega_2 F_{2\gamma} ,
\end{aligned} \tag{7}$$

where σ_1, σ_2, and σ_3 are subshell photoionization cross sections of the elements at the excitation energies; ω_1, ω_2, and ω_3 are L-subshell fluorescence yields; f_{12}, f_{13}, and f_{23} are the Coster-Kronig transition probabilities; and F_{ny} (F_{3l}, $F_{3\alpha}$, $F_{3\beta}$, etc.) are the fractions of the radiation width of the subshell L_η ($L_{\rm I}$, $L_{\rm II}$, and $L_{\rm III}$) contained in

TABLE II. Theoretical L-subshell fluorescence yields, Coster-Kronig yields, and partial radiative widths used in this work.

	L-subshell fluorescence yields[a]			L-subshell Coster-Kronig yields[a]		
Target	ω_1	ω_2	ω_3	f_{12}	f_{13}	f_{23}
Pb	0.112	0.373	0.360	0.12	0.58	0.116
Au	0.107	0.334	0.320	0.14	0.53	0.122
Yb	0.112	0.222	0.210	0.19	0.29	0.138
Ho	0.094	0.189	0.182	0.19	0.30	0.142
Pr	0.061	0.117	0.118	0.19	0.29	0.153

	Partial radiative widths[b]						
Target	$F_{1\gamma}$	$F_{2\gamma}$	$F_{1\beta}$	$F_{2\beta}$	$F_{3\beta}$	$F_{3\alpha}$	F_{3l}
Pb	0.2316	0.189	0.7355	0.789	0.180	0.777	0.0419
Au	0.2270	0.180	0.7466	0.798	0.172	0.787	0.0404
Yb	0.2116	0.153	0.7718	0.825	0.149	0.815	0.0368
Ho	0.2115	0.152	0.7744	0.826	0.148	0.816	0.0355
Pr	0.2085	0.146	0.7814	0.830	0.143	0.822	0.0329

[a]Reference [7].
[b]References [16] and [17].

TABLE III. Uncertainties in the quantities used to determine L x-ray fluorescence cross sections in Eq. (1).

Quantity	Nature of uncertainty	Uncertainty (%)
I_i, N_i $(i=l,\alpha,\beta,\gamma)$	statistical plus peak stripping	<3
$I_0 G \epsilon_{Li}$	errors in different parameters used to evaluate this factor	<3
t	nonuniform thickness and other random experimental errors	<3
β	error in the absorption coefficients at incident and emitted energies	negligible

the yth spectral line, i.e.,

$$F_{ny}=\Gamma_{ny}/\Gamma \quad (F_{3\alpha}=\Gamma_{3\alpha}/\Gamma_3) \; . \tag{8}$$

Here, Γ_3 is the theoretical total radiative transition rate of the $L_{\rm III}$ shell and $F_{3\alpha}$ is the sum of the radiative transition rates that contribute to the $L\alpha$ lines associated with hole filling in the $L_{\rm III}$ shell; that is,

$$\Gamma_{3\alpha}=\Gamma_3(M_{\rm IV}-L_{\rm III})+\Gamma_3(M_{\rm V}-L_{\rm III}) \quad \text{where } \Gamma_3(M_{\rm IV}-L_{\rm III}) \tag{9}$$

is the radiative transition rate from the $M_{\rm IV}$ shell to the $L_{\rm III}$ shell. The radiative transition rates for many elements have been calculated by Scofield, who applied the relativistic Hartree-Slater theory with a central potential and included the retardation effect. The values of all the atomic parameters used in our measurements are presented in Table II.

The overall error in the measured L x-ray fluorescence cross sections is estimated to be less than 8%, which arises due to the uncertainties in the various physical parameters required to evaluate the experimental results using Eq. (1). The uncertainties in all the parameters are listed in Table III. It is evident from Table I that the present experimental values are higher than the theoretical estimates for all the elements when the semiempirically fitted ω_i and f_{ij} tabulated values are used in the calculation of theoretical L x-ray fluorescence cross sections. The errors in the tabulated values of L-subshell fluorescence yields are 3–15 %, and the errors in the values of L-subshell Coster-Kronig transition probabilities f_{ij} are 10–20 %. These uncertainties in ω_i and f_{ij} can give rise to an error more of than 20% in the final values of the theoretical L x-ray fluorescence cross sections.

The disagreement between the experimental and theoretical results can either be due to some systematic error in the experimental measurements or an error in calculating the physical parameters (σ_{Li} and/or F_{ny}) used to evaluate the theoretical L x-ray fluorescence cross sections.

Theoretical values of L-subshell photoionization cross sections have been taken from the latest available tabulations. These tabulated values have a calculational error of less than 0.1%. No experimental results for L-subshell photoionization cross sections are available. Also, experimental and theoretical results of total-atom photoionization cross sections above 100 keV are in agreement, with an uncertainity of a few percent [20].

The values of parameters such as fluorescence yield and emission rates need to be measured accurately. These parameters—based on relativistic Dirac-Hartree-Slater theory—need to be calculated for all the elements in question in order to check the validity of the theory in this atomic region. However, for trace-elemental analysis using a fundamental parameter approach, one should use experimental values of L x-ray fluorescence cross sections since they involve an error of less than 8%, whereas, theoretical values of L x-ray fluorescence cross sections can have an error of up to 20%. L x-ray fluorescence cross sections need to be measured using more elements covering a wider range of energy.

TABLE IV. Comparison of experimental and theoretical L-shell intensity ratios at photon energies E (keV).

		$I_{Li}/I_{L\alpha}$		$I_{L\beta}/I_{L\alpha}$		$I_{L\gamma}/I_{L\alpha}$	
Target	E	Expt.	Theor.	Expt.	Theor.	Expt.	Theor.
Pb	23.62	0.047±0.004	0.054	1.028±0.048	0.9662	0.1697±0.008	0.1825
	24.68	0.047±0.004	0.054	1.023±0.046	0.9922	0.1898±0.010	0.1884
Au	23.62	0.048±0.004	0.051	1.045±0.044	1.0176	0.1776±0.012	0.1773
	24.68	0.049±0.004	0.051	1.059±0.046	1.0385	0.1768±0.010	0.1802
Yb	23.62	0.045±0.004	0.045	1.137±0.040	1.1144	0.2139±0.012	0.2002
	24.68	0.045±0.004	0.045	1.060±0.038	1.1350	0.2112±0.007	0.2148
Ho	23.62	0.045±0.004	0.045	1.082±0.039	1.0508	0.1854±0.007	0.1839
	24.68	0.045±0.004	0.045	1.072±0.034	1.0744	0.1852±0.008	0.1890
Pr	23.62			1.055±0.042	1.0331	0.1743±0.009	0.1791
	24.68			1.076±0.050	1.0537	0.1753±0.010	0.1880

The relative intensities can be obtained from the L x-ray fluorescence cross-section data, but the error will increase in quadrature and will be around 10%. In view of this, the errors in the intensity ratios have been calculated using Eq. (6). As a result, the error in the measured relative intensity ratios is reduced to 3–6 %. The experimentally calculated intensity ratios using Eq. (6) have been compared with the theoretical values in Table IV. The intensity ratios for intense transitions, $I_{L\beta}/I_{L\alpha}$, are in good agreement with the theoretical values.

ACKNOWLEDGMENTS

We are very grateful to Professor Dr. G. Furlan for providing financial assistance, and to the Centro Interdipartimentale di Ricerca per l'Analisi dei Modelli e dell'Informazione nei Sistemi Biomedici for allowing us to carry out this experimental work. One of us (D.V.R.) undertook this work with the support of the International Centre for Theoretical Physics (ICTP) Program for Training and Research in Italian Laboratories, Trieste, Italy.

[1] C. N. Chang and W. H. Su, Nucl. Instrum. Methods **148**, 561 (1978).
[2] K. Shatendra, K. Allawadhi, and B. S. Sood, Phys. Rev. A **31**, 2918 (1985).
[3] K. S. Mann, R. Mittal, K. L. Allawadhi, and B. S. Sood, Phys. Rev. A **44**, 2198 (1991).
[4] R. L. Watson, M. W. Michael, J. Hernandez, A. K. Leaper, and C. D. Wendt, Adv. X-ray Anal. **21**, 105 (1978).
[5] J. H. McCrary, L. V. Singman, L. H. Ziegler, L. D. Looney, C. M. Edmonds, and C. E. Harris, Phys. Rev. A **5**, 1587 (1972).
[6] S. I. Salem, S. L. Panossion, and R. A. Krause, At. Data Nucl. Data Tables **14**, 91 (1974).
[7] M. O. Krause, C. W. Nestor, C. J. Sparks, Jr., and E. Ricci, Oak Ridge National Laboratory Report No. ONRL-5399 (1978) (unpublished).
[8] M. H. Chen, B. Crasemann, and V. O. Kostroun, Phys. Rev. A **4**, 1 (1971).
[9] B. Crasemann, M. H. Chen, and V. O. Kostroun, Phys. Rev. A **4**, 2161 (1971).
[10] M. H. Chen, B. Crasemann, and H. Mark, Phys. Rev. A **24**, 177 (1981).
[11] R. Cesareo, in *Nuclear Analytical Techniques in Medicine,* edited by R. Cesareo (Elsevier, Amsterdam, 1988), pp. 19–121.
[12] P. Standzenieks and E. Selin, Nucl. Instrum. Methods **165**, 63 (1979).
[13] M. R. Khan and M. Karimi, X-ray Spectrometry **9**, 32 (1980).
[14] E. Strom and I. Israel, Nucl. Data Tables A **7**, 565 (1970).
[15] J. H. Scofield, University of California Radiation Laboratory Report No. 51326 (Lawrence Livermore National Laboratory) (1973) (unpublished).
[16] J. H. Scofield, Phys. Rev. A **179**, 9 (1969).
[17] J. H. Scofield, At. Data Nucl. Data. Tables **14**, 121 (1974).
[18] D. A. Close, R. C. Bearse, J. J. Malanify, and J. J. Umberger, Phys. Rev. A **8**, 1873 (1973).
[19] G. A. Bissinger, A. B. Baskin, B. H. Choi, S. M. Shafroth, T. M. Howard, and A. W. Waltener, Phys. Rev. A **6**, 545 (1972).
[20] R. H. Pratt, Ron Akiva, and H. K. Tseng, Rev. Mod. Phys. **45**, 273 (1973).